JOURNAL OF APPLIED ELECTROCHEMISTRY 21 (1991) 793–798

Behaviour of a carbon felt flow by electrodes Part I: Mass transfer characteristics

R. CARTA, S. PALMAS, A. M. POLCARO, G. TOLA

Dipartimento di Ingegneria Chimica e Materiali, Universita' di Cagliari, Piazza d'Armi, 09123 Cagliari, Italy

Received 8 October 1990; revised 17 March 1991

The properties of a carbon felt electrode have been experimentally investigated with special attention to its possible application in the electrochemical recovery of heavy metals. The mass transfer process has been studied by means of the reduction of ferricyanide and cupric ions for a flow-by electrode operating under limiting current conditions. An empirical correlation between the Sherwood and Reynolds numbers has been used to compare the experimental data with those obtained by other authors for different porous electrodes.

Notation

a	specific electrode area (m^{-1})
a_V	area per unit solid volume (m^{-1})
C_{in}	entering concentration of reacting species ($kmol\,m^{-3}$)
C_{out}	exit concentration of reacting species ($kmol\,m^{-3}$)
d_f	fibre diameter (m)
d_h	hydraulic diameter of the felt fibres (m)
D	diffusion coefficient ($m^2\,s^{-1}$)
F	Faraday number 96487 ($C\,mol^{-1}$)
k_m	mass transfer coefficient ($m\,s^{-1}$)
I_{lim}	limiting current (A)
l	length of the electrode (m)
L	thickness of the electrode (m)
Q_L	catholyte flow rate ($m^3\,s^{-1}$)
Re	Reynolds number $Re = d_h u/v$
Sh	Sherwood number $Sh = k_m d_h/D$
u	solution velocity in the empty cross-section ($m\,s^{-1}$)
X	reaction conversion
z	number of electrons in the electrochemical reaction

Greek letters

θ	porosity of the felt
v	kinematic viscosity of the solution ($m^2\,s^{-1}$)
ρ_R, ρ_A	true and apparent density of the felt ($kg\,m^{-3}$)

1. Introduction

The study of porous electrodes is a matter of increasing interest in several fields such as power storage and new electro-organic synthesis. Their application has also been suggested for the recovery of several heavy metal pollutants from dilute solutions [1, 2].

Among the different materials, carbon felts have provided promising results [3] owing to their favourable physico-chemical characteristics: high chemical stability, large specific surface area, good fluid permeability and high electric conductivity, together with continuity of the electronic contact throughout the electrode.

This work presents a contribution to the studies of the mass transfer characteristics, which play an important role in the electrodeposition of metals, for a carbon felt electrode in a flow-by configuration. Such an arrangement (i.e. with the current flow perpendicular to that of the electrolyte) has been adopted to allow the use of an electrode that is thin in the current direction and long in the flow direction so that a high product conversion is achieved and a more or less uniform distribution of the potential inside the bed is maintained [4].

2. Experimental details

2.1. *Electrode material*

Carbon felt (SIGRI Gmbh) was used for the flow-by electrode. Scanning electron microscopy showed an anisotropic texture of cylindrical fibres furrowed by shallow grooves (Fig. 1a,b). No significant microporosity was detected in the fibres. The value for their diameter, d_f, was obtained from an average of numerous measurements from micrographs.

The overall porosity, θ, was calculated as $\theta = (\rho_R - \rho_A)/\rho_R$ where ρ_R is the true density of the

Table 1. Physical properties of the felt

Fibre diameter	d_f	$(11.0 \pm 0.5) \times 10^{-6}$ m
Apparent density	ρ_A	$122\,kg\,m^{-3}$
True density	ρ_R	$2100\,kg\,m^{-3}$
Porosity	θ	0.94

0021-891X/91 $03.00 + .12

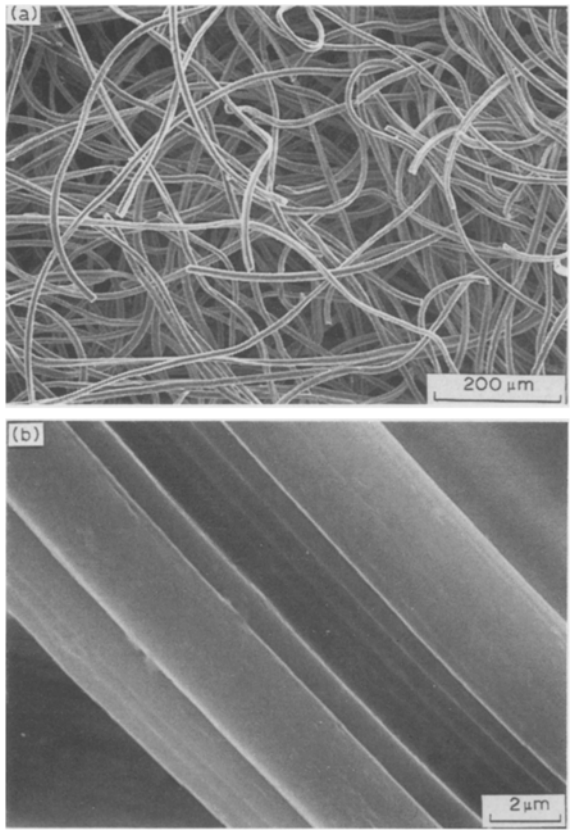

Fig. 1. Scanning electron micrographs for carbon felt: (a) material texture; (b) details of the fibre.

sample, determined by means of a helium pycnometer and ρ_A is the apparent density measured with a mercury pycnometer. The physical properties of the felt are summarized in Table 1.

2.2. *Apparatus and procedure*

A flow-cell made of Teflon® was used to perform the electrochemical measurements. Figure 2 shows a schematic view of the cell and of the hydraulic circuit. The cell comprised two compartments (width 2 cm, thickness 0.5 cm, length 4 cm) separated by a porous glass disc. In each compartment there was a calming zone at the electrolyte inlet and a case where a felt strip (width 2 cm, thickness 0.5 cm, length 1–2 cm) was held (Fig. 2a). The electrical contact was made by a thin platinium sheet connected to a potentiostat-galvanostat (EG & G mod. 273) able to correct the data automatically for ohmic resistance by the current interruption method.

The reference electrode was a satured calomel electrode connected to the working electrode through a Luggin probe which fitted the back side of the felt. All the potential values given in the text are referred to this electrode. The mass transfer characteristics of the carbon felt were studied by means of the reduction of ferricyanide ions and cupric ions. In the former case the electrolytes were solutions of $K_3Fe(CN)_6$

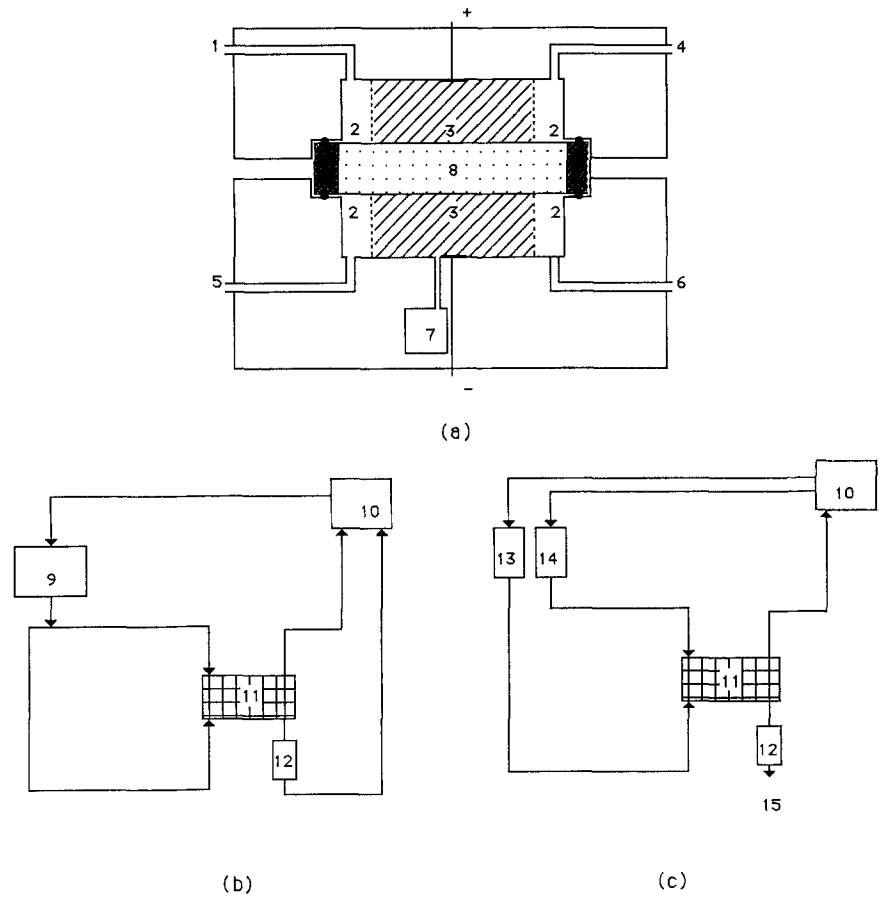

Fig. 2. Schematic view of the cell (a) and of the hydraulic circuit (b, c): 1. anolyte inlet; 2. calming zone; 3. electrode; 4. anolyte outlet; 5. catholyte inlet; 6. catholyte outlet; 7. reference electrode; 8. porous glass disc; 9. reservoir; 10. peristaltic pump; 11. cell; 12. flowmeter; 13. catholyte reservoir; 14. anolyte reservoir; 15. samples.

Table 2. Composition and properties of the electrolyte

Composition	5×10^{-4}i2 $\times 10^{-3}$ M $K_3Fe(CN)_6$ 0.1 M $K_4Fe(CN)_6$ 1 M KNO_3	5×10^{-4}i1 $\times 10^{-3}$ M $CuSO_4$ 0.1 M H_2SO_4
Kinematic viscosity	$\nu = 0.914 \times 10^{-6}$ m^2 s^{-1}	$\nu = 1.024 \times 10^{-6}$ m^2 s^{-1}
Diffusion coefficient of relevant ions	$D = 7.6 \times 10^{-10}$ m^2 s^{-1}	$D = 7.5 \times 10^{-10}$ m^2 s^{-1}
Conductivity	$\gamma_0 = 8.8\,\Omega^{-1}$ m^{-1} [4] $\gamma = 8.1\,\Omega^{-1}$ m^{-1}	$\gamma_0 = 9.2\,\Omega^{-1}$ m^{-1} $\gamma = 8.4\,\Omega^{-1}$ m^{-1}
Schmidt number	1203	1365

and $K_4Fe(CN)_6$ in KNO_3 as supporting electrolyte (Table 2). A high ratio between $K_4Fe(CN)_6$ and $K_3Fe(CN)_6$ concentrations was used to avoid oxygen evolution and current limitations at the anode. Figure 2b shows the hydraulic circuit used. The electrolyte was recirculated by means of a preset peristaltic pump by means of which the liquid was recirculated to the reservoir to dampen oscillations in the electrolyte flow-rate. The electrolyte entering the cell was split into two streams and the flow leaving the cathodic compartment was measured by means of a rotameter. Both streams were returned to the electrolyte storage so that the initial concentration was restored. Potassium ferricyanide concentration was determined by an iodometric titration method with an accuracy of $\pm 1\%$. The limiting currents were determined from measurements of current-voltage curves obtained by applying a linear voltage scan of 0.5 mV s^{-1} to the electrochemical cell.

The study of the mass transfer characteristics for the reduction of cupric ions was performed using dilute solutions of $CuSO_4$ in H_2SO_4 (Table 2). These solutions were pumped throughout the cathodic compartment at a preset flow-rate. A solution of sulphuric acid flowed in the closed anodic circuit. The hydraulic circuit is represented in Fig. 2c. A preliminary analysis of the anolyte showed that the concentration of Cu^{2+} was zero, at least within the experimental accuracy, assuring that during the run the diffusion through the porous disc was already negligible. The current-voltage curves were obtained by increasing the potential of the cathode stepwise starting from the open circuit potential: at each increment the current was measured after the steady state had been reached. At this time the solution leaving the cathodic compartment was sampled for Cu^{2+} concentration analysis and subsequent samples were taken until a constant value was achieved. All the analyses were made with an Atomic Absorption Spectrophotometer (IL Video12); triple distilled water and AnalaR grade reagents were used for the solutions. Before each run the solutions were deaerated by bubbling nitrogen. All the runs were performed at 25 $\pm$ 0.1° C.

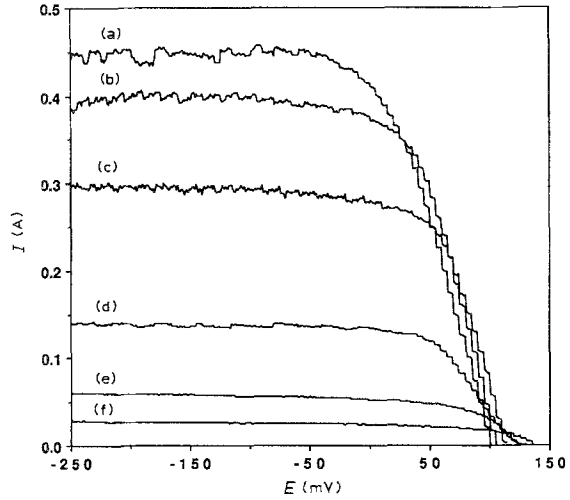

Fig. 3. Polarization curves for the reduction of ferricyanide ions in solution of 2×10^{-3} M $K_3Fe(CN)_6$, 0.1 M $K_4Fe(CN)_6$, 1 M KNO_3 at several electrolyte velocities, u: (a) 8.1×10^{-2}; (b) 5.8×10^{-2}; (c) 3.7×10^{-2}; (d) 1.3×10^{-2}; (e) 0.55×10^{-2}; (f) 0.39×10^{-2} m s^{-1}.

3. Results and discussion

In Fig. 3 a few typical current-potential curves at steady-state for the flow-by carbon felt electrode in solutions of $K_3Fe(CN)_6$ are shown. The curves give a well defined value of the limiting current (I_{lim}) so that the reaction conversion, X, can be obtained, given a Faradic efficiency of one, using the relationship

$$X = \frac{I_{lim}}{zFQ_L C_{in}} \tag{1}$$

where Q_L is the electrolyte flow-rate and C_{in} the entering reactant concentration.

Figure 4 shows a few experimental current-potential curves for the cathodic reduction of Cu^{2+} in H_2SO_4 at fixed Cu^{2+} inlet concentration and different electrolyte velocities. As can be seen an appreciable distortion of the limiting current plateau appears, therefore the conversion for the cathodic reduction of Cu^{2+} under diffusion control was calculated as

$$X = \frac{C_{in} - C_{out}}{C_{in}} \tag{2}$$

The C_{out} value was measured with the cathode at such a potential that the exit concentration no longer depended on the electrode potential.

From the values of X the effective mass transfer coefficient was calculated as [5]

$$ak_m = -\frac{u}{l} \ln (1 - X) \tag{3}$$

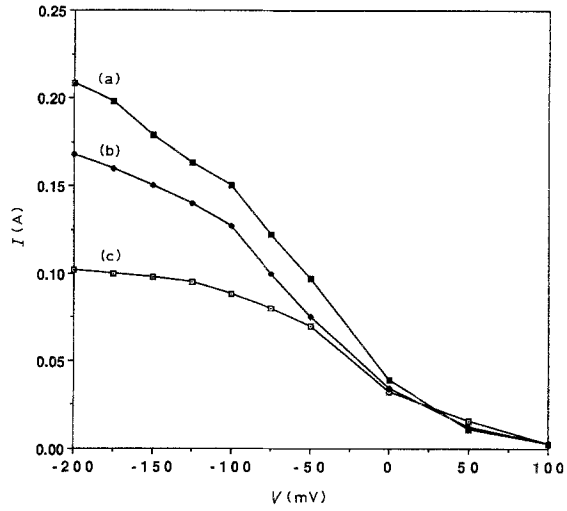

Fig. 4. Current values against electrode potential for the system 1×10^{-3} M $CuSO_4$, 0.1 M H_2SO_4 at several electrolyte velocities, u: (a) 4×10^{-2}; (b) 2×10^{-2}; (c) 1×10^{-2} m s^{-1}.

where a is the specific electrode area, u is the linear velocity of the electrolyte in the empty cross-section and l is the length of the electrode.

Figure 5 shows ak_m values obtained for the reduction of ferricyanide ions and cupric ions. At higher velocities the data for both systems agree well, show only a small scatter and do not depend on the electrode length as dictated by Equation 3. Therefore beyond 0.5×10^{-2} m s^{-1} plug flow conditions are actually verified and Equation 3 gives the true mass transfer coefficient from the bulk of the solution in the pores to the fibre surface. At the low velocities the values of ak_m show large scatter: however it must be noted that for X close to 1 small uncertainties in its evaluation give a large variation of ak_m. Moreover at the low velocities the ak_m values are smaller for $[Cu^{2+}]$ reduction as compared with those for $[Fe(CN)_6]^{-3}$. This behaviour suggests that the large crystals of metal, which grow mostly at the inlet of the felt bed under these conditions, may cause a blocking effect which is dominant relative to the surface area enhancement.

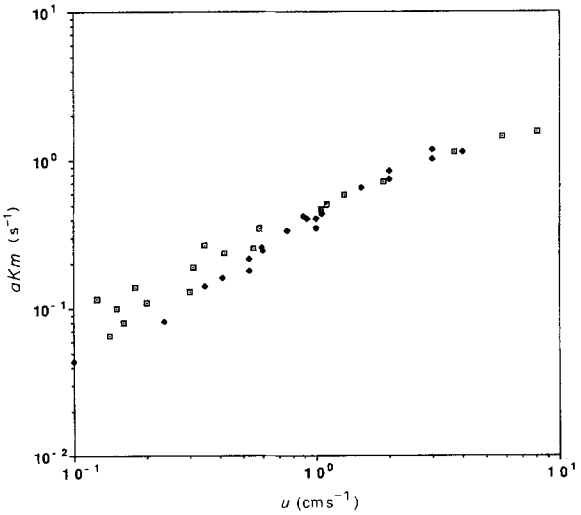

Fig. 5. Experimental ak_m values against electrolyte velocity: □ data from $[Fe(Cn)_6]^{-3}$ reduction; ◆ data from $[Cu^{2+}]$ reduction.

Mass transfer data in flow systems are usually represented in the form Sh = constant $Re^{\alpha}Sc^{\beta}$. A similar correlation has been utilized for porous bed electrodes consisting of graphite particles [6] and for reticulated three dimensional electrodes [7]. Different approaches can be used to define the specific area, a, and the characteristic dimension, d_h, needed for the calculation of these dimensionless numbers from the experimentally accessible product ak_m. In this work d_h is defined as [8, 9]:

$$d_h = 4\theta/a \tag{4}$$

Evaluation of the true interfacial area available for the reaction is uncertain, [10]. Different results are obtained according to whether the physical method utilized provides only the surface due to the interstices between the fibres, which enable free flow of solution or the overall surface area including that given by the microporosity. Moreover, it has been pointed out [11] that, whereas the whole specific area is the only important parameter when the electrochemical reaction is kinetically limited, a strong effect of pore size distribution is obtained when the reaction is diffusion controlled. In the present case a geometrical approach seems to give suitable results for evaluating the area per unit volume (a_v) because of the uniform diameter of the cylindrical fibres (see Fig. 1b); taking into account the electrode porosity, the specific area may be calculated as:

$$a = a_v(1 - \theta) = \frac{4}{d_f}(1 - \theta) \tag{5}$$

From the data of this work the correlation $Sh = 3.19\,Re^{0.69}$ was obtained, using for d_f and θ the values reported in Table 1. In this correlation the Schmidt number, that for flow systems usually appears to the power 1/3, was included in the constant term of the equation because its value was very close for both the solutions considered (Table 2).

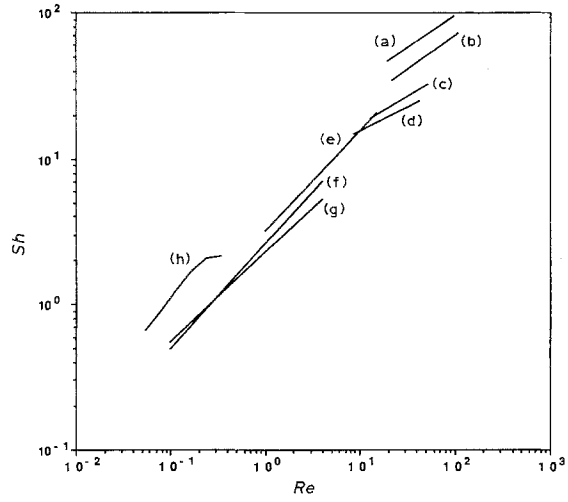

Fig. 6. *Re–Sh* correlation for various porous electrode materials. (a) Nickel spheres: $d = 0.002\,\mu$m, $\theta = 0.4$ [4, 14]; (b) nickel foam: $a = 3500\,m^{-1}$, $\theta = 0.978$ [13]; (c) nickel foam: $a = 5750\,m^{-1}$, $\theta = 0.975$ [13]; (d) nickel foam: $a = 9250\,m^{-1}$, $\theta = 0.973$ [13]; (e) carbon felt [this work]; (f) carbon felt: $d_f = 25.4\,\mu$m, $\theta = 0.90$ [12]; (g) carbon felt: $d_f = 25.4\,\mu$m, $\theta = 0.86$ [12]; (h) reticulate vitreous carbon: $\theta = 0.97$, $a = 6600\,m^{-1}$ [1].

In Fig. 6 this correlation is compared with those obtained for different materials by other authors [1, 4, 12–14]. In all these cases, the equivalent diameter, defined in Equation 4, is used as characteristic dimension. The specific area was evaluated using the geometrical approach for felts and for fixed beds of spheres, whereas for Ni foams the area obtained according to the Ergun equation was used, as suggested by the authors themselves [13]. Also in this case $Sc^{1/3}$ was included in the constant term, because its variation was in the range 10.13 [4]–11.62 [10, 13]. It may be noted that such representation gives results in excellent agreement for all the felts examined and is capable of giving a good interpretation of mass transfer characteristics for very widely different geometrical configurations.

From the ak_m data it is possible to evaluate the potential distribution in the bed due to the ohmic drop in the electrolyte. For instance Storck *et al.* [4] have developed a model considering a reactor with a flow-by electrode in which the main reaction was diffusion controlled, no secondary reaction occurred and plug flow conditions were assumed. Their results show that the potential drop, $\Delta\eta$, through the bed thickness was largest at the inlet of the bed and decreased with axial distance. The relationship obtained at the inlet section was

$$\Delta\eta_{max} = \frac{ak_m}{2\gamma} zFC_0L^2 \qquad (6)$$

where L is the electrode thickness and γ is the apparent conductivity inside the pores, related to the electrolyte conductivity, γ_0, by the equation

$$\gamma = \gamma_0\left(\frac{2\theta}{3-\theta}\right) \qquad (7)$$

For the electrode studied in this work low values of $\Delta\eta_{max}$ occur, over a large range of experimental conditions, because the solution inside the pores has a conductivity similar to that in the bulk, owing to the high felt porosity. For instance for $C_0 = 5 \times 10^{-4}$ M, $u = 10^{-2}$ m s^{-1} and the γ values reported in Table 2 we obtain $\Delta\eta_{max} = 30$ mV and 52 mV for the systems with ferricyanide and copper, respectively.

Moreover, in a flow by regime it is possible to maintain $\Delta\eta_{max}$ within the maximum variation allowable to avoid secondary reactions using a low electrode thickness. Nevertheless, the distortion of the limiting current plateau observed in all the experimental conditions for the system $CuSO_4/H_2SO_4$ (see Fig. 4) may be explained by postulating a simultaneous reaction at the electrode. Indeed a small amount of dissolved hydrogen may be generated even if the potential does not reach the reversible potential for HER at 1 atm, required for gas bubble evolution. The formation of hydrogen at more positive potentials than that of reversible hydrogen has also been reported for other porous electrodes such as PTFE-bounded platinum fuel cell electrodes [5]. In that case the effect was attributed to the formation of hydrogen at very low partial pressure, due to the porous electrode structure permitting a very rapid diffusion of hydrogen away from the electrode surface.

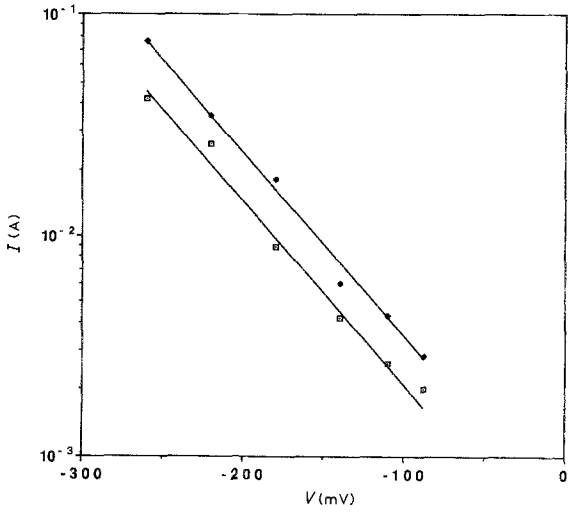

Fig. 7. Tafel curves in 0.1 M H_2SO_4 solutions: (◆) carbon felt electrode with a copper deposit ($V_{dep} = -250$ mV for 200 s); (⊡) carbon felt.

Figure 7 shows a Tafel curve obtained at a felt electrode with only 0.1 M H_2SO_4 compared with that at a felt where Cu was previously deposited from a solution of 10^{-3} M $CuSO_4$ in 0.1 M H_2SO_4. In both cases a straight line plot of log I against E was obtained: the shift toward higher current values observed at the electrode with a Cu deposit suggests that the metal layer on the carbon fibres enhances the exchange current for dissolved hydrogen formation.

The importance of the exchange current of the secondary reaction on the distortion of the limiting current plateau was pointed out in the work of White and Newman [16] and Trainham and Newman [17] where copper deposition with simultaneous dissolved hydrogen production was investigated at a rotating and at a flow-through porous electrode, respectively.

4. Conclusions

The results obtained in the present work confirm the good mass transfer performance of the carbon felt electrode studied. Moreover the high porosity of the felt allows a high electrolyte conductivity inside the pores and thus, if the electrolyte has a sufficiently high conductivity, the ohmic drop remains low for a wide range of experimental conditions. These features make it a very efficient electrode material for use in electrochemical heavy metal recovery from solutions with high conductivity and also in cases of very low metal concentration.

Experimental studies are continuing with the intention of improving the mass transfer correlation at the low velocities needed to achieve a near-complete metal recovery with an acceptable electrode length. Other studies are also necessary to evaluate the maximum amount of metal that can be deposited on the electrode without causing a significant reduction in the mass transfer efficiency.

Acknowledgement

The authors wish to thank Dr A. Ibba, Dipartimento di Scienza della Terra Universita' di Cagliari, for kindly supplying the scanning electron micrographs.

References

[1] M. Matlosz and J. Newman, *J. Electrochem. Soc.* **133** (1986) 1850.
[2] R. E. Sioda and H. Piotrowska, *Electrochim. Acta* **25** (1980) 331.
[3] Y. Oren and A. Soffer, *ibid.* **28** (1983) 1649.
[4] A. Storck, M. A. Enriquez-Granados, M. Roger and F. Coeuret, *ibid.* **27** (1982) 293.
[5] P. W. Appel and J. Newman, *AIChE J.* **22** (1976) 979.
[6] F. Coeuret, *Electrochim. Acta* **21** (1976) 185.
[7] A. Tentorio and V. Casolo-Ginelli, *J. Appl. Electrochem.* **8** (1978) 195.
[8] B. G. Ateya, *ibid.* **16** (1980) 627.
[9] H. H. P. Skelland, 'Diffusional Mass Transfer' Wiley & Sons, New York (1974).
[10] S. Langlois and F. Coeuret, *J. Appl. Electrochem.* **19** (1989) 43.
[11] J. Jorne and E. Roayaie, *J. Electrochem. Soc.* **133** (1986) 1649.
[12] K. Kinoshita and S. C. Leach, *ibid.* **129** (1982) 1993.
[13] S. Langlois and F. Coeuret, *J. Appl. Electrochem.* **19** (1989) 51.
[14] M. A. Enriquez-Granados, D. Hutin and A. Stork, *Electrochimica Acta* **27** (1982) 303.
[15] J. Giner, J. M. Parry, S. Smith and M. Turchan, *J. Electrochem. Soc.* **116** (1969) 1692.
[16] R. White and J. Newman, *J. Electroanal. Chem.* **82** (1977) 173.
[17] J. A. Trainham and J. Newman, *J. Electrochem. Soc.* **124** (1977) 1528.